Inorganic Chemistry
Article

Inorg. Chem. **2010**, *49*, 8421–8429 **8421**
DOI: 10.1021/ic100952q

Ligand Effects on the $[Cu(PhO)(PhOH)]^+$ Redox Active Complex

Elixabete Rezabal,[†] Lucie Ducháčková,[‡] Petr Milko,[§] Max C. Holthausen,*[,†] and Jana Roithová*[,‡]

[†]*Institut für Anorganische und Analytische Chemie, Johann Wolfgang Goethe-Universität Frankfurt, Max-von-Laue-Strasse 7, 60438 Frankfurt am Main, Germany,* [‡]*Department of Organic and Nuclear Chemistry, Faculty of Science, Charles University in Prague, Hlavova 8, 12840 Praha 2, Czech Republic, and* [§]*Institute of Organic Chemistry and Biochemistry, Flemingovo nám. 2, 16610 Prague 6, Czech Republic*

Received May 13, 2010

Under gas phase conditions, the $[Cu(PhO)(PhOH)]^+$ complex is composed of copper(I), a phenoxy radical bound via the oxygen atom, and a phenol bound via the aromatic ring. Effects of additional ligand coordination on the molecular and electronic structure of the complex $[Cu(PhO)(PhOH)]^+$ are investigated by mass spectrometric and quantum chemical means for $[Cu(PhO)L]^+$ (L = H_2O, CH_3OH, tetrahydrofuran, NH_3, pyridine, imidazole, 1,2-dimethoxyethylene, *N*,*N*,*N*′,*N*′-tetramethylethylenediamine, pyrrole, and thiophene) and $[Cu(PhO)(PhOH)L_n]^+$ (L = H_2O, NH_3, and 4-methylimidazole) models. The nature and number of additional ligands critically influences the spin distribution in the complex, which is sensitively reflected by the phenoxy CO stretching mode.

Introduction

Copper enzymes play a key role in electron transfer processes, in the metabolism of dioxygen, in the deactivation of toxic intermediates of O_2 reduction, and within the biological nitrogen cycle. The various functions of copper proteins are controlled by an intimate interplay between ligands and/or solvent molecules around the copper center[1−4] and its redox properties. The copper ions primarily occur in the two oxidation states +I and +II, which are easily accessible under physiological conditions.[5−15] Particular interest has been devoted to the structure/reactivity interplay in the radical copper oxidases, a family of enzymes with very similar active sites, which perform a diverse array of biological functions. These enzymes combine a copper ion and a stable protein free radical site (e.g., formed from a covalently cross-linked tyrosine-cysteine dimer in the case of galactose oxidase) as redox centers in an efficient catalytic unit, which accomplishes a two-electron oxidation of simple alcohols to aldehydes along with the reduction of O_2 to hydrogen peroxide.[16] The galactose oxidase active site contains a metal coordinated by four protein ligands, that is, two tyrosine and two histidine groups in an approximately square pyramidal coordination geometry (Scheme 1).[17−19] The search for synthetic analogues as models for its structure, spectroscopy, and reactivity has led to bioinspired complexes that replicate several features of the active site.[20−22]

We have recently studied a simplistic gas phase model composed of a copper(II) ion, a phenol (PhOH), and a phenolate ligand (PhO^-) by mass spectrometric and quantum chemical means.[23] In the resulting complex $[Cu(PhO)(PhOH)]^+$ the coordination of phenolate to copper(II) was found to be

*To whom correspondence should be addressed. E-mail: roithova@natur.cuni.cz (J.R.), max.holthausen@chemie.uni-frankfurt.de (M.C.H.).

(1) Pasquarello, A.; Petri, I.; Salmon, P. S.; Parisel, O.; Car, R.; Tóth, E.; Powell, D. H.; Fischer, H. E.; Helm, L.; Merbach, A. E. *Science* **2001**, *291*, 856.
(2) Chaboy, J.; Munoz-Paez, A.; Merkling, P. J.; Marcos, E. S. *J. Chem. Phys.* **2006**, *124*, 064509.
(3) Inoue, K.; Ohashi, K.; Iino, T.; Judai, K.; Nishi, N.; Sekiya, H. *Phys. Chem. Chem. Phys.* **2007**, *9*, 4793.
(4) Blumberger, J.; Bernasconi, L.; Tavernelli, I.; Vuilleumier, R.; Sprik, M. *J. Am. Chem. Soc.* **2004**, *126*, 3928.
(5) Kaim, W. *Dalton Trans.* **2003**, *5*, 761.
(6) Kaim, W.; Schwederski, B. *Bioinorganic Chemistry: Inorganic Elements in the Chemistry of Life: An Introduction and Guide*; Meyer, G., Nakamura, A., Eds.; John Wiley & Sons Ltd.: London, 2001; pp 187−214.
(7) Solomon, E. I.; Chen, P.; Metz, M.; Lee, S.-K.; Palmer, A. E. *Angew. Chem., Int. Ed.* **2001**, *40*, 4570.
(8) Holm, R. H.; Kennepohl, P.; Solomon, E. I. *Chem. Rev.* **1996**, *96*, 2239.
(9) Kaim, W.; Raall, J. *Angew. Chem., Int. Ed.* **1996**, *35*, 43.
(10) Malmstrom, B. G. *Eur. J. Biochem.* **1994**, *223*, 711.
(11) Williams, R. J. P. *Eur. J. Biochem.* **1995**, *234*, 363.
(12) Blackburn, N. J.; Rhames, F. C.; Ralle, M.; Jaron, S. J. *Biol. Inorg. Chem.* **2000**, *5*, 341.
(13) Gray, H. B.; Malmstrom, B. G.; Williams, R. J. P. *J. Biol. Inorg. Chem.* **2000**, *5*, 551.
(14) Solomon, E. I.; Szilagyi, R. K.; DeBeer George, S.; Basumallick, L. *Chem. Rev.* **2004**, *104*, 419.
(15) Ghosh, S.; Xie, X. J.; Dey, A.; Sun, Y.; Scholes, C. P.; Solomon, E. I. *Proc. Natl. Acad. Sci. U.S.A.* **2009**, *106*, 4969.
(16) Whittaker, J. W.; Whittaker, M. M. *Pure Appl. Chem.* **1998**, *70*, 903.
(17) Ito, N.; Philips, S. E. V.; Yadav, K. D. S.; Knowles, P. F. *J. Mol. Biol.* **1994**, *238*, 794.
(18) Whittaker, M. M.; Kersten, P. J.; Cullen, D.; Whittaker, J. W. *J. Biol. Chem.* **1999**, *274*, 36226.
(19) Whittaker, M. M. *Chem. Rev.* **2003**, *103*, 2347.
(20) Rothlisberger, U.; Carloni, C. *Int. J. Quantum Chem.* **1999**, *73*, 209.
(21) Thomas, F. *Eur. J. Inorg. Chem.* **2007**, 2379.
(22) Jazdzewski, B. A.; Tolman, W. B. *Coord. Chem. Rev.* **2000**, *200*−*202*, 633.
(23) Milko, P.; Roithová, J.; Schröder, D.; Lemaire, J.; Schwarz, H.; Holthausen, M. *Chem.—Eur. J.* **2008**, *14*, 4318.

Published on Web 08/20/2010

Scheme 1. Schematic Drawing of the Active Center of Galactose Oxidase (GO) Interacting with a Substrate[a]

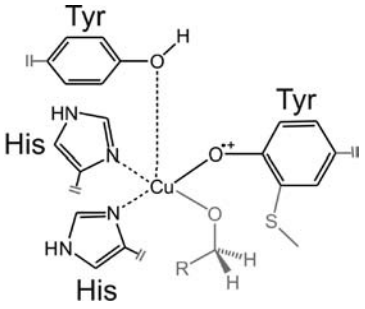

[a] Part in black represents the studied model. Note that the active form of the GO contains the copper(II)/phenoxy unit, which is in the resting state reduced to copper(II)/phenolate.

associated with an electron transfer, and the resulting species corresponds to copper(I) coordinated to the oxygen atom of a phenoxy radical, which carries an unpaired electron localized at the aromatic ring. The neutral phenol ligand then binds to this complex preferentially by the π-electrons of the aromatic ring. Subsequent work on alternative complexes $[Cu(PhO)L]^+$ indicated that addition of the monodentate ligands L = NH_3, H_2O, and pyridine has only a small effect on the structure and spin distribution of the $[Cu(PhO)]^+$ core.[24] However, as soon as the number of monodentate ligands exceeds one, or a bidentate ligand like *N*,*N*,*N*′,*N*′-tetramethylethylenediamine (TMEDA) is coordinated, the electronic structure of the resulting complex is changed and corresponds rather to a Cu^{II} complex with a phenolate counterion, and the remaining ligand(s). It was shown that the number ligands of *n* crucially influences the electron distribution and, consequently, the Cu oxidation state in the complexes $[Cu(PhO)L_n]^+$, but the electronic structure of the $[Cu(PhO)]^+$ moiety was found rather insensitive to the nature of the ligands attached.

In the present study we extend this work to a larger set of ligands L in complexes of the type $[Cu(PhO)(PhOH)L_n]^+$ (n = 1,2). Energy resolved dissociation mass spectrometry and quantum chemical calculations are used to provide a more detailed view on the structural and electronic properties of such species. Our aim is to show the effect of additional ligands on the properties of $[Cu(PhO)(PhOH)]^+$ and thus to illustrate the transition from our simplistic model toward systems more resembling Cu sites in enzymes. We, however, do not aim at the precise theoretical description of the active site of galactose oxidase itself.[25]

Experimental and Computations Details

The experiments are performed with a TSQ Classic mass spectrometer with a QOQ configuration (Q stands for quadrupole and O stands for octopole) described in detail elsewhere.[26,27] The ions of interest were generated by electrospray ionization (ESI) from aqueous solutions of $Cu(NO_3)_2$, phenol, and the ligands (methanol, tetrahydrofuran (THF), thiophene, imidazole, pyrrole, pyridine, *N*,*N*,*N*′,*N*′-tetramethylethylenediamine (TMEDA), or 1,2-dimethoxyethylene (DME)) or from aqueous solution of $CuBr_2$, phenol, and NH_3. The first quadrupole is used to record source spectra or to mass-select the desired ions. The mass-selected ions are collided with argon or xenon ($p_{Ar} \cong 0.1$ mTorr, $p_{Xe} \cong 0.08$ mTorr) in the octopole collision cell, and the fragments are analyzed by Q2. The collision energy can be varied by changing the potential offset between Q1 and O. The energy scale was determined by means of the retarding potential analysis; the energy resolution was 1.2 ± 0.1 eV in the laboratory frame (full width at half-maximum). Appearance energies (AEs) of various fragmentation channels can be determined from the dependence of their relative cross sections on the collision energy.[28−30] The relative cross sections are evaluated using the L-CID program,[28] which has originally been developed for thermalized ions. Our experimental setup does not allow for thermalization, however, which means that the ions generated carry an undetermined internal energy exceeding the assumed thermal energy. As a result, the binding energies determined are expected to be systematically lower than those predicted by theory. To account for a broader internal-energy distribution than expected for the thermalized ions, we have set a kinetic-energy distribution of the parent ions to 2 eV and considered a temperature of 200 °C instead of the actual temperature of the collision cell (40 °C). All parameters used for the fitting are given in detail in the Supporting Information.

The theoretical binding energies were obtained by performing geometry optimizations at the B3LYP[31] level, employing the TZVP[32] basis set as implemented in the Gaussian 03 package.[33] Harmonic vibrational frequencies and zero point vibrational energies (ZPVEs) were computed at the same level of theory. Energies reported refer to enthalpy changes ΔH at 0 K, which were obtained as the sum of total energies and ZPVE contributions. Additional calculations were performed with the Orca program[34] at the B3LYP-D/TZVP level, employing Grimme's empirical correction for dispersion.[35]

Results and Discussion

Effects of Additional Ligands on the $[Cu(PhO)]^+$ Complex. The $[Cu(PhO)L]^+$ complexes were generated by

(24) Milko, P.; Roithová, J.; Tsierkezos, N.; Schröder, D. *J. Am. Chem. Soc.* **2008**, *130*, 7186.
(25) For theoretical investigations of galactose-oxidase active site see: (a) Himo, F.; Eriksson, L. A.; Maseras, F.; Siegbahn, P. E. M. *J. Am. Chem. Soc.* **2000**, *122*, 8031. (b) Rokhsana, D.; Dooley, D. M.; Szilagyi, R. K. *J. Am. Chem. Soc.* **2006**, *128*, 15550. (c) Rokhsana, D.; Dooley, D. M.; Szilagyi, R. K. *J. Biol. Inorg. Chem.* **2008**, *13*, 371.
(26) Experiments with xenon as collision gas: (a) Roithová, J.; Schröder, D. *Phys. Chem. Chem. Phys.* **2007**, *9*, 731. (b) Roithová, J.; Schröder, D.; Míšek, J.; Stará, I. G.; Starý, I. *J. Mass Spectrom.* **2007**, *42*, 1233.
(27) Experiments with argon as collision gas: Ducháčková, L.; Roithová, J. *Chem.—Eur. J.* **2009**, *15*, 13399.
(28) Narancic, S.; Bach, A.; Chen, P. *J. Phys. Chem. A* **2007**, *111*, 7006.
(29) Armentrout, P. B.; Ervin, K. M.; Rodgers, M. T. *J. Chem. Phys.* **2008**, *112*, 10071.
(30) Schröder, D.; Engeser, M.; Brönstrup, M.; Daniel, C.; Spandl, J.; Hartl, H. *Int. J. Mass Spectrom.* **2003**, *228*, 743.
(31) (a) Becke, A. D. *Phys. Rev. A* **1988**, *38*, 3098. (b) Lee, C.; Yang, W.; Parr, R. *Phys. Rev. B* **1988**, *37*, 785. (c) Becke, A. D. *J. Chem. Phys.* **1993**, *98*, 5648. (d) Stephens, P. J.; Devling, F. J.; Chabalowski, C. F.; Frisch, M. J. *J. Phys. Chem.* **1994**, *98*, 11623.
(32) (a) Schaefer, A.; Horn, H.; Ahlrich, R. *J. Chem. Phys.* **1992**, *97*, 2571. (b) Schaefer, A.; Huber, C.; Ahlrichs, R. *J. Chem. Phys.* **1994**, *100*, 5829.
(33) Frisch, M. J.; Trucks, G.W.; Schlegel, H.B.; Scuseria, G.E.; Robb, M.A.; Cheeseman, J.R.; Montgomery, J.A.; , Jr., Vreven, T.; Kudin, K.N.; Burant, J.C.; Millam, J.M.; Iyengar, S.S.; Tomasi, J.; Barone, V.; Mennucci, B.; Cossi, M.; Scalmani, G.; Rega, N.; Petersson, G.A.; Nakatsuji, H.; Hada, M.; Ehara, M.; Toyota, K.; Fukuda, R.; Hasegawa, J.; Ishida, M.; Nakajima, T.; Honda, Y.; Kitao, O.; Nakai, H.; Klene, M.; Li, X.; Knox, J.E.; Hratchian, H.P.; Cross, J.B.; Bakken, V.; Adamo, C.; Jaramillo, J.; Gomperts, R.; Stratmann, R.E.; Yazyev, O.; Austin, A.J.; Cammi, R.; Pomelli, C.; Ochterski, J.W.; Ayala, P.Y.; Morokuma, K.; Voth, G.A.; Salvador, P.; Dannenberg, J.J.; Zakrzewski, V. G.; Dapprich, S.; Daniels, A.D.; Strain, M.C.; Farkas, O.; Malick, D.K.; Rabuck, A.D.; Raghavachari, K.; Foresman, J.B.; Ortiz, J.V.; Cui, Q.; Baboul, A.G.; Clifford, S.; Cioslowski, J.; Stefanov, B.B.; Liu, G.; Liashenko, A.; Piskorz, P.; Komaromi, I.; Martin, R.L.; Fox, D.J.; Keith, T.; M. A. Al-Laham, Peng, C. Y.; Nanayakkara, A.; Challacombe, M.; Gill, P.M.W.; Johnson, B.; Chen, W.; Wong, M.W.; Gonzalez, C.; Pople, J.A. *Gaussian 03*, Revision C.02; Gaussian, Inc.: Wallingford, CT, 2004.
(34) Neese, F. *ORCA*, Revision 2.6.35; Universität Bonn: Bonn, Germany, 2008.
(35) Grimme, S. *J. Comput. Chem.* **2006**, *27*, 1787.

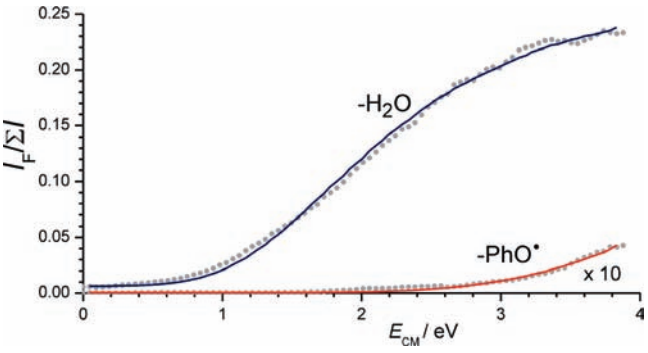

Figure 1. L-CID fits of the energy resolved collision induced dissociation of $[Cu(PhO)(H_2O)]^+$ (collision gas: argon). Number of degrees of freedom is 42, number of free rotations 3, and the transition states for eliminations of water and the phenoxy radical are set as loose.

Table 1. Experimental and Theoretical Bond-Dissociation Energies (BDE_{exp} and BDE_{theor}) of PhO and L in the $[Cu(PhO)(L)]^+$ Complexes

	BDE_{exp} (eV)		BDE_{theor} (eV)	
L	-PhO	-L	-PhO	-L
H_2O	2.5 ± 0.3	1.5 ± 0.3	2.45	1.67
CH_3OH	2.2 ± 0.2	1.4 ± 0.2	2.41	1.81
THF	2.1 ± 0.2	1.9 ± 0.2	2.09	2.07
thiophene	2.0 ± 0.2	1.7 ± 0.2	1.91	1.77
NH_3	1.9 ± 0.2	1.9 ± 0.2	2.13	2.30
pyrrole	1.9 ± 0.2	2.1 ± 0.2	1.84	2.26
pyridine	2.0 ± 0.2	2.1 ± 0.2	2.23	2.54
imidazole	2.0 ± 0.2	2.4 ± 0.2	2.22	2.76
DME	1.7 ± 0.2	2.0 ± 0.2	1.73	2.18
TMEDA	1.7 ± 0.2	(2.3 ± 0.3)[a]	1.72	3.17

[a] The energy corresponds to the formation of iminium ion from the TMEDA ligand and thus not to a loss of TMEDA.

electrospray ionization of aqueous solutions of copper salt, ligand, and phenol. Binding energies between copper and the phenoxy, *BDE*(PhO), and between copper and the other ligand, *BDE*(L), were estimated based on the energy-resolved collision-induced dissociation. The dependence of the relative fragmentation cross sections on the collision energy can be evaluated by various methods. We applied the L-CID program of Chen and co-workers, which does not require input from quantum chemical calculations for the investigated dissociations. The input parameters necessary for the fitting procedure include the kinetic-energy resolution of a parent ion, the number of degrees of freedom of the parent ion, the number of free rotors in the parent ion (single bonds with free rotations), and information whether the transition state for the dissociation is loose or tight. With respect to the fragmentations, which represent a simple cleavage of a bond between copper and a ligand, we have assigned the supposed transition states as loose. An example of the L-CID fitting of the energy-dependent cross sections is shown for the $[Cu(PhO)(H_2O)]^+$ (Figure 1), and the results for all $[Cu(PhO)(L)]^+$ complexes (L = H_2O, CH_3OH, THF, thiophene, NH_3, pyrrole, pyridine, imidazole, DME, and TMEDA) are summarized in Table 1. Estimation of the experimental errors is based on the quality of the experimental data and several independent fittings with the L-CID program. Further details can be found in the Supporting Information.

For each $[Cu(PhO)(L)]^+$ complex included in the experimental study several coordination modes were investigated by quantum chemical means. The most stable complex geometries are shown in Figure 2, and the corresponding properties are summarized in Table 2.

The clear preference of the phenoxy ligand to bind to copper via the oxygen atom has already been established in a previous work,[23] and we will therefore not discuss this binding mode further here. Most of the monodentate ligands investigated preferentially coordinate via a heteroatom lone pair to copper, including pyridine and imidazole for which alternative π coordination modes are energetically disfavored by more than 1 eV (cf. Supporting Information). For pyrrole and thiophene, instead, bonding through the π system is favored over σ coordination modes by 0.45 and 0.09 eV, respectively (cf. Supporting Information, Figure S9).

Both sets of *BDE*s (see Table 1) agree with the mass spectrometric measurements within the experimental error bars, with the notable exception of *BDE*(L) for the N-donor ligands NH_3, pyridine, and imidazole, which exceed the upper experimental limit by up to 0.24 eV. As alluded to above, we attribute these discrepancies to the lacking thermalization of the parent ions in our experiment, which render the experimentally obtained *BDE*s too low.

Although the nature of the ligand L evidently has a significant influence on the *BDE*, the spin distributions within the $[Cu(PhO)]^+$ fragments remain essentially unaltered for all complexes $[Cu(PhO)L]^+$ bearing monodentate ligands L. Mulliken analyses performed for these complexes show that the unpaired electron is essentially localized at the phenoxy ligand, and only negligible spin densities reside on the copper ion and the ligand L (Table 2). A shift of the spin population toward Cu is in fact only observed to some extent (0.108 and 0.221 unpaired electrons on Cu, respectively) for the bidentate ligands DME and TMEDA.

The fragment charge distributions show larger variations, and Figure 3 shows a clear correlation between the binding energy of a ligand L to the $[Cu(PhO)]^+$ complex with the charge population at the ligand L. Obviously, an increase of the binding energy is associated with an increase of the ligand charge, which reflects the ability of the ligand L to compensate the charge deficit of the $[Cu(PhO)]^+$ fragment. Following expectations, the ligands coordinated via a harder oxygen atom are less strongly bound to the soft Cu^I ion compared to the softer nitrogen donor ligands. While NH_3 still is a poor electron-donor ligand, the larger binding energies of pyridine and imidazole are a consequence of additional bonding contributions by the π-system of these ligands (see Supporting Information). Substantial deviations from the linear correlation between the fragment charge and the binding energies occur only for the two π-bound ligands pyrrole and thiophene.

Effects of Additional Ligands on the $[Cu(PhO)(PhOH)]^+$ Complex. Our previous investigation of the structure and electronic properties of $[Cu(PhO)(PhOH)]^+$ showed that the most stable isomer contains an O-bound phenoxy radical and a π coordinated phenol group, a binding situation which by and large corresponds to the binding modes discussed for the complexes $[Cu(PhO)(pyrrole)]^+$ and $[Cu(PhO)(thiophene)]^+$ in the previous section.[23] This π coordination mode of phenol, however, is not in accordance with the O-bound phenol coordination mode reported for structures of the copper radical oxidase active sites. We attributed this discrepancy to the presence of further ligands at the enzyme

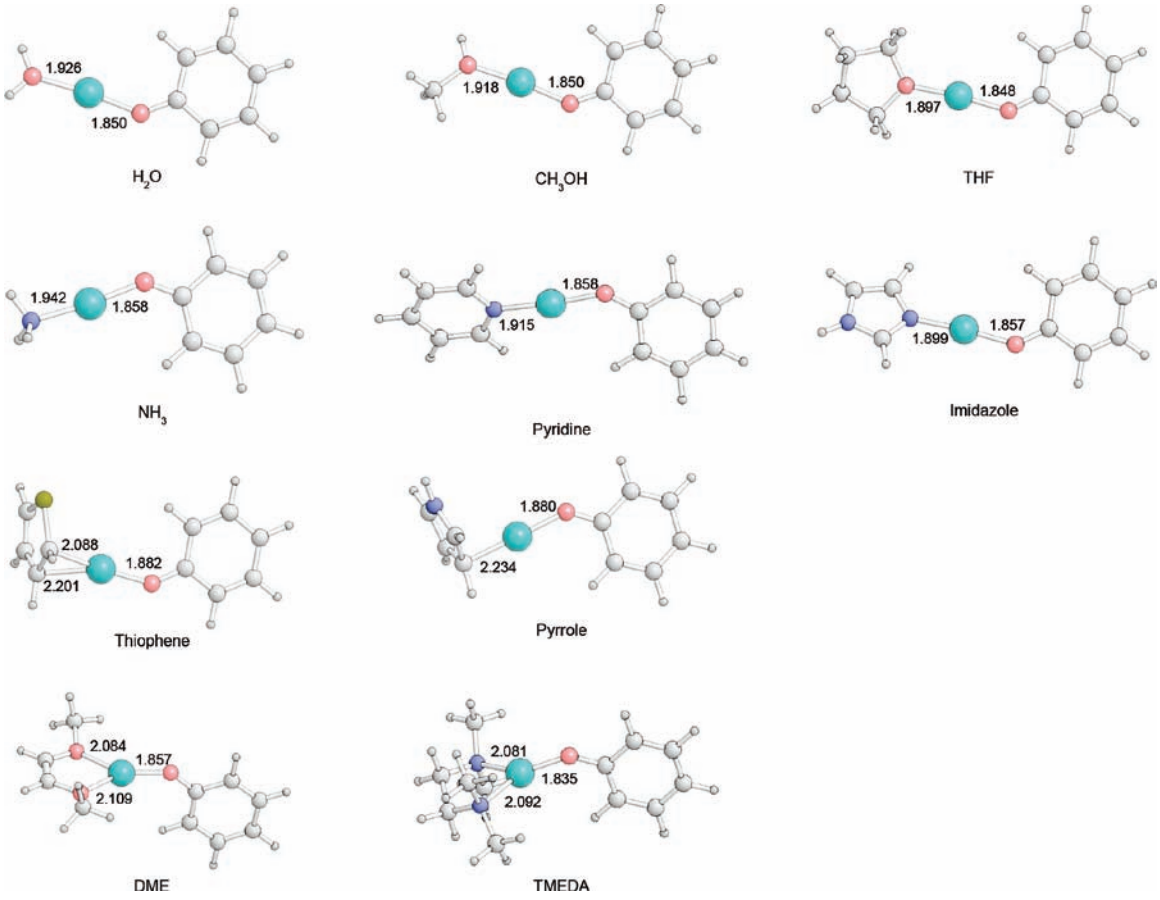

Figure 2. Coordination modes of most stable $[Cu(PhO)(L)]^+$ isomers (bond distances given in Å).

Table 2. Computed Parameters for $[Cu(PhO)(L)]^+$ Complexes (B3LYP/TZVP Level)

	bond length (Å)		$s(X)^a$				$q(X)^b$			Cu sd hybrid	
L	Cu−O	Cu−L	X = Cu	X = O	X = Ph	X = L	X = Cu	X = PhO	X = L	%4s/%3d	$\nu(CO)^c$
H_2O	1.850	1.926	0.028	0.297	0.674	0.001	0.55	0.27	0.18	91/9	1508
CH_3OH	1.850	1.918	0.032	0.300	0.667	0.002	0.53	0.26	0.21	91/9	1505
THF	1.848	1.897	0.041	0.305	0.651	0.004	0.52	0.25	0.23	91/9	1513
thiophene	1.882	2.145	0.021	0.299	0.677	−0.002	0.35	0.25	0.40	94/6	1512
NH_3	1.858	1.942	0.027	0.300	0.674	−0.001	0.45	0.27	0.29	90/10	1510
pyrrole	1.880	2.234	0.032	0.308	0.654	−0.001	0.37	0.24	0.39	93/6	1503
pyridine	1.858	1.915	0.035	0.305	0.660	−0.001	0.43	0.25	0.32	90/10	1505
imidazole	1.857	1.899	0.041	0.309	0.649	−0.001	0.40	0.25	0.36	91/9	1502
DME	1.857	2.097	0.108	0.318	0.563	0.005	0.57	0.15	0.28	95/4	1372
TMEDA	1.835	2.086	0.221	0.294	0.396	0.043	0.48	−0.02	0.54	96/4	1322

[a] Spin densities determined by Mulliken population analysis. [b] Charge densities determined by Mulliken population analysis. [c] Harmonic frequencies, not scaled (cm^{-1}).

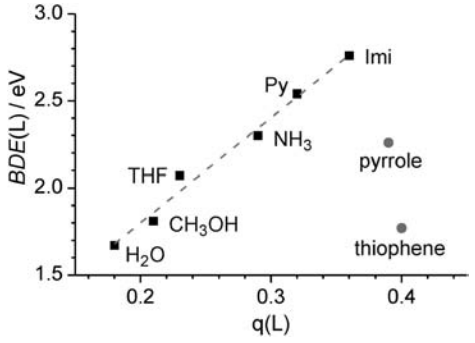

Figure 3. Binding energies between $[Cu(PhO)]^+$ and a monodentate ligand L as a function of partial charge localized at the ligand L.

active sites, which obviously induce a change in the phenol coordination mode. We furthermore expect that the presence of additional ligands might lead to alterations in the spin distribution, eventually affecting the oxidation state of the metal. In this section, we study the changes introduced to the electronic structures of complexes formed by addition of one or two further ligands L to the $[Cu(PhO)(PhOH)]^+$ core with L = NH_3, H_2O, and 4-methylimidazole (Imi_{Me}). The particular choice of 4-methylimidazole as ligand is motivated by the analogy with the model of the enzymatic active center (see Scheme 1).

The structures of the four $[Cu(PhO)(PhOH)]^+$ isomers identified previously (see Figure 4)[23] were taken as starting points for the sequential addition of further ligands.

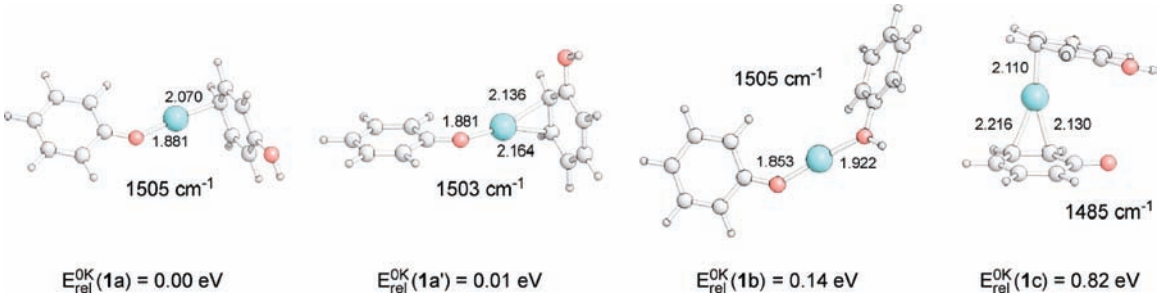

Figure 4. Isomers of the complex $[Cu(PhO)(PhOH)]^+$ (ZPVE corrected energies relative to **1**a; bond distances in angstrom; C−O stretching modes of the phenoxy ligands in wavenumbers).

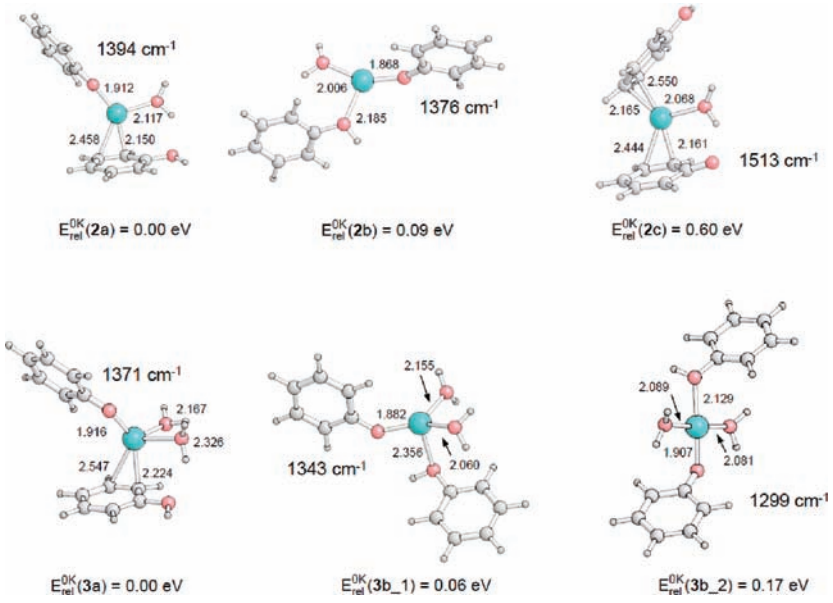

Figure 5. Most stable isomers of the complexes $[Cu(PhO)(PhOH)(H_2O)_n]^+$ ($n = 1, 2$) (ZPVE corrected energies relative to **2**a and **3**a, respectively; bond distances in angstrom; C−O stretching modes of the phenoxy ligands in wavenumbers).

The nomenclature presented in Figure 4 will be maintained in the following discussion: an index "a" denotes isomers in which the core complex contains phenol coordinated via the aromatic ring and the phenoxy group via the oxygen atom. An index "b" stands for isomers in which both, PhOH and PhO, are O-bound and an index "c" is used for isomers in which both ligands are coordinated via the aromatic rings. A variety of isomers have been identified in the calculations for the resulting complexes but to keep the discussion concise, only the most stable isomers will be discussed below. Higher energy isomers, including those with second coordination shell ligands, are presented in the Supporting Information.

$[Cu(PhO)(PhOH)(H_2O)]^+$ isomers resulting from the addition of one molecule of water to the structures **1**a−c are shown in Figure 5. The relative isomer energies closely follow the trends observed for **1**a−c, but energy differences are less pronounced. Isomers **2**a and **2**b, which differ in the coordination of neutral phenol, are almost isoenergetic, whereas **2**c lies 0.60 eV higher in energy. Several isomers of **2**a have been located, which differ in the coordination of the aromatic phenol ring, but all have relative energies within 0.08 eV (cf. Supporting Information, Figure S11). This is in agreement with the view of a nearly free "copper-ring walk" already mentioned in our previous work, that is, the different π-bound structures coexist in a dynamic equilibrium. For comparison, the effect of Grimme's empirical correction on the relative energies of **2**a−c is estimated by a single-point calculations at the B3LYP-D/TZVP level (Table 3). Although the order of the isomer stabilities stays the same, the relative energies of the π-bonded structures decrease. As a result, the energy difference between **2**a and **2**b increases to 0.16 eV, whereas the difference between **2**a and **2**c decreases to 0.45 eV.

Upon coordination of the second molecule of water to form $[Cu(PhO)(PhOH)(H_2O)_2]^+$, a spontaneous migration of one water molecule to the second solvation sphere occurs (see Supporting Information). This points to the preference for the tris-coordination of copper in the complex. The energy difference between the isomers with phenol bonded via the aromatic ring and the oxygen atom (**3**a and **3**b, respectively) is about the same as found for **2**a and **2**b, and no minimum for isomer **3**c could have been localized. The isomers **3**b_1 and **3**b_2 differ in the geometry arrangements of the ligands around copper. The more stable isomer **3**b_1 has a tetrahedral arrangement of the ligands, which is typical for copper(I) complexes, whereas the isomer **3**b_2 has a square planar geometry preferred by copper(II) complexes.

Table 3. Computed Binding Energies of Ligands L in the $[Cu(PhO)(PhOH)(L)_n]^+$ Complexes[a]

				BE (eV)		*BE*(+*D*) (eV)
L	*n*	isomer	Δ*E* (eV)	-L	Δ*E*(+*D*) (eV)	-L
H_2O	1	**2**a	0.00	0.50	0.00	0.64
		2b	0.09	0.41	0.16	0.48
		2c	0.60	−0.11	0.45	0.19
	2	**3**a	0.00	0.87[b]	0.00	1.16
		3b_1	0.06	0.82[b]	0.16	1.00
		3b_2	0.17	0.70[b]	0.22	0.94
NH_3	1	**4**a	0.07	0.84	0.00	1.04
		4b	0.00	0.90	0.05	0.99
		4c	0.68	0.23	0.43	0.61
Imi_{Me}	1	**5**a	0.10	1.25	0.00	1.51
		5b	0.00	1.35	0.03	1.49
		5c	0.69	0.66	0.33	1.18
	2	**6**b	0.00	2.38[b]	0.00	2.78

[a] Geometries were optimized at the B3LYP/TZVP level. The energies were further refined by a single point calculation at the B3LYP-D/TZVP level; these values are denoted as (+*D*). [b] Values refer to sum of binding energies of both molecules of L.

A detailed analysis of the electronic structures of the isomers of **2** and **3** reveals that in all cases the spin population is dominantly localized at the phenoxy moiety (Table 4). The energetically higher lying isomer **2**c contains both, the phenol and the phenoxy ligands in a π coordination mode, and represents a limiting case. The C−O stretching mode above 1500 cm^{-1} is typical for a phenoxy radical[36] which clearly implies a formal oxidation state of +I for the copper ion in this complex. The isomer **3**b_2 can be identified as a counter pole with a significant increase in spin population at the copper ion and the C−O stretching mode below 1300 cm^{-1}. On the basis of its square planar coordination geometry and its low C−O stretching frequency, we conclude that this isomer represents a Cu(II) complex. The remaining complexes present a gradual change between the two limiting cases.

Addition of one ammonia molecule to **1**a−c results in structures analogous to the water complexes (Figure 6). The isomers with π coordinated (**4**a) and the oxygen-coordinated (**4**b) phenol are almost isoenergetic. Thus, while the B3LYP calculation slightly energetically prefers the isomer **4**b (by 0.07 eV), the B3LYP-D method provides the isomer **4**a as the most stable one (by 0.05 eV). We also found a set of energetically close lying isomers in which ammonia replaces phenol, expelling it into the second coordination sphere (cf. Supporting Information, Figure S12). Addition of two ammonia ligands led in all cases to only tricoordinated complexes with either ammonia or phenol bound in a second coordination sphere (cf. Supporting Information, Figure S12). Comparison of charge and spin population distributions of the ammonia complexes **4**a−c with their counterparts **2**a−c reveals by and large a very similar picture. The only significant difference visible is an increased positive charge population present at the NH_3 fragments compared to the corresponding complexes of water ligands, which we attribute to the larger electron-donor capacity of the ammonia ligands. At the same time, charge populations at the phenol ligands are smaller in the ammonia complexes than in the water complexes, and the effect is strongest for the "a" isomers. In line with these findings, the slightly longer metal−carbon bond distances to the π coordinated phenol in **4**a indicate a weaker bonding compared to **2**a (cf. Figures 5 and 6). To some minor extent a corresponding effect is also visible for the O coordinated phenol ligands in **4**b and **2**b.

Finally, coordination of one 4-methylimidazole ligand leads to complexes **5**a−c with a relative energy ordering almost identical to that found for ammonia complexes (Figure 7). Addition of a second 4-methylimidazole yields a tetracoordinated complex **6**b with a σ(O) bound phenol ligand. Attempts to localize a corresponding isomer **6**a resulted in structures with phenol bound in the second solvation sphere. This is consistent with the proposed destabilization of π phenol binding modes by stronger N-donor ligands. The close resemblance of the results of the Mulliken spin analysis, as well as the very low computed C−O stretching mode of the PhO ligand with complex **3**b_2, identifies **6**b as a Cu(II) complex. As **3**b_2, however, exhibits a square planar coordination geometry we searched for corresponding isomers of **6**b. We were able to localize several corresponding structures, which are, however, several eV less stable than **6**b. To account for potential stabilizing $\pi-\pi$ interactions in the aromatic ligand environment we repeated these calculations employing Grimme's empirical correction scheme in B3LYP-D/TZVP calculations. But although these contributions stabilize these isomers by about 0.4 eV, all such species are less stable than **6**b by at least 2.50 eV (cf. Supporting Information, Figure S13). We thus conclude that **6**b represents a quasi-tetrahedral Cu(II) complex, somewhat mimicking related Cu(II) coordination geometries in the active sites of copper enzymes.

A pertinent question stems from the discrepancy between the spin distribution in seemingly analogous complexes **3**b_1 and **6**b. Both complexes have tetrahedral arrangement of ligands around copper, but the former represents a copper(I) complex, whereas the latter is a copper(II) complex. Comparison of charge distributions in the complexes reveals that the water ligands in **3**b_1 carry a positive-charge population of 0.25 e, which is much less than a population of 0.67 e localized at the 4-methylimidazole ligands of **6**b (Table 4). The remaining positive charge is mostly localized at the copper ion. The large positive charge (+0.61 e) on copper in **3**b_1 is thus most probably responsible for the oxidation of the phenoxy ligand. In comparison, the $[Cu(PhO)(PhOH)(Imi_{Me})_2]^+$ (**6**b) complex copper bears a charge population of only +0.44 e. This in other words means that under the same geometry confinement, stronger electron-donor ligands reduce the $Cu^{I/II}$ redox potential and therefore favor the copper(II)/phenolate form. In the less stable isomer **3**b_2 of $[Cu(PhO)(PhOH)(H_2O)_2]^+$, the charge population on the copper ion is also large (+0.66 e), but the copper(II) oxidation state is probably stabilized by the tetragonal arrangement of the ligands.

A comparison of results for all complexes $[Cu(PhO)(PhOH)(L)_n]^+$ investigated confirms our previous finding that the electronic structure of copper/phenoxy complexes is crucially influenced by the number and nature of additional ligands. According to spin population and the CO stretching mode, the complexes are divided into three groups.

(36) Sokolowski, A.; Leutbecher, H.; Weyhermüller, T.; Schnepf, R.; Both, E.; Bill, E.; Hildebrandt, P.; Wieghardt, K. *J. Biol. Inorg. Chem.* **1997**, *2*, 444.

Table 4. B3LYP/TZVP Computed Parameters for $[Cu(PhO)(PhOH)(L)_n]^+$ Complexes[a]

			$s(X)$[a]			$q(X)$[b]				Cu sd hybrid	
L	*n*	isomer	X = Cu	X = O	X = Ph	X = Cu	X = PhO	X = PhOH	X = L	%4s/%3d	ν(CO)[c]
H_2O	1	**2**a	0.066	0.325	0.601	0.47	0.17	0.25	0.11	97/3	1394
		2b	0.103	0.318	0.568	0.58	0.15	0.12	0.14	95/5	1376
		2c	0.080	0.336	0.575	0.33	0.22	0.31	0.14	98/1	1513
	2	**3**a	0.116	0.327	0.540	0.49	0.10	0.23	0.18	98/1	1371
		3b_1	0.190	0.311	0.485	0.61	0.06	0.07	0.25	98/2	1343
		3b_2	0.360	0.270	0.320	0.66	−0.10	0.14	0.29	98/2	1299
NH_3	1	**4**a	0.091	0.319	0.559	0.42	0.14	0.20	0.25	95/5	1374
		4b	0.077	0.318	0.597	0.48	0.18	0.09	0.25	93/7	1390
		4c	0.080	0.334	0.562	0.26	0.19	0.30	0.25	98/1	1520
Imi_{Me}	1	**5**a	0.121	0.320	0.521	0.37	0.09	0.20	0.34	96/4	1360
		5b	0.120	0.320	0.545	0.46	0.12	0.08	0.34	94/6	1369
		5c	0.081	0.336	0.553	0.17	0.22	0.25	0.35	98/2	1520
	2	**6**b	0.378	0.259	0.281	0.44	−0.16	0.05	0.67	99/1	1302

[a] Spin densities determined by Mulliken population analysis. [b] Charge densities determined by Mulliken population analysis. [c] Unscaled harmonic frequencies in cm^{-1}.

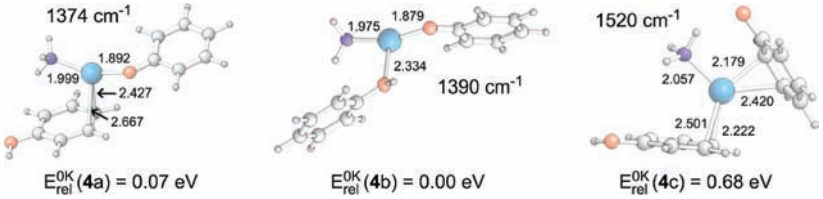

Figure 6. Most stable isomers of the $[Cu(PhO)(PhOH)(NH_3)]^+$ complex (ZPVE corrected energies relative to **4**b; bond distances in angstrom; C−O stretching modes of the phenoxy ligands in wavenumbers).

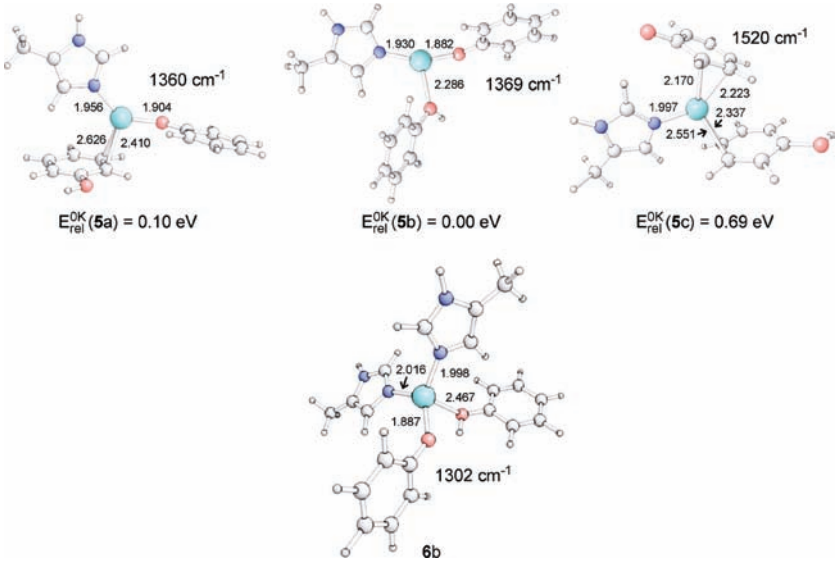

Figure 7. Most stable isomers of the complexes $[Cu(PhO)(PhOH)(Imi_{Me})_n]^+$ (n = 1, 2) (ZPVE corrected energies for isomers of **5** relative to **5**a; bond distances in angstrom; C−O stretching modes of the phenoxy ligands in wavenumbers).

The first group is constituted from the "c" isomers, which contain a phenoxy radical and copper(I). The corresponding C−O stretching frequency is found above 1500 cm^{-1} as it is typical for the phenoxy radicals.[36] For the second group, the C−O stretching frequency (cf. Table 4) is red-shifted to the range between 1340 and 1400 cm^{-1}, but the spin population is still dominantly localized at the phenoxy ligand. These species can be also viewed as complexes of copper(I). In agreement with the expected preference of soft (Cu^I)−soft (π-electron system) interaction, all isomeric complexes with neutral phenol coordinated via the aromatic ring belong to these two groups. The last group of complexes is composed from the tetracoordinate $[Cu(PhO)(PhOH)(Imi_{Me})_2]^+$ complex **6**b and the square planar $[Cu(PhO)(PhOH)(H_2O)_2]^+$ isomer **3**b_2. In both complexes the spin population is almost equally shared between the phenoxy ligand and the copper ion. Together with the low C−O stretching frequency of about 1300 cm^{-1} our results indicate that a formal Cu(II) oxidation state should be assigned for these two complexes. Accordingly, these complexes bear phenol coordinated via the harder oxygen atom.

Table 5. Spin Densities[a] at $[Cu(PhO)(PhOH)(L)_n]^+$ Calculated with Different Density Functionals[b]

			BHandHLYP//B3LYP			B38P86//B3LYP			B38P86		
L	*n*	isomer	X = Cu	X = O	X = Ph	X = Cu	X = O	X = Ph	X = Cu	X = O	X = Ph
H_2O	1	**2**a	0.008	0.377	0.602	0.024	0.356	0.616	0.015	0.342	0.640
		2b	0.017	0.377	0.602	0.044	0.355	0.596	0.020	0.332	0.646
		2c	0.036	0.424	0.537	0.052	0.381	0.561	0.049	0.376	0.568
	2	**3**a	0.019	0.403	0.574	0.050	0.374	0.569	0.027	0.356	0.612
		3b_1	0.049	0.403	0.581	0.113	0.364	0.514	0.066	0.352	0.577
		3b_2	0.556	0.235	0.150	0.410	0.282	0.255	0.618	0.190	0.080
NH_3	1	**4**a	0.014	0.383	0.594	0.039	0.358	0.586	0.024	0.349	0.616
		4b	0.010	0.370	0.618	0.030	0.349	0.617	0.015	0.333	0.651
		4c	0.036	0.432	0.520	0.054	0.384	0.545	0.053	0.379	0.551
Imi_{Me}	1	**5**a	0.023	0.400	0.565	0.057	0.368	0.553	0.019	0.363	0.610
		5b	0.021	0.392	0.582	0.053	0.363	0.576	0.029	0.348	0.618
		5c	0.032	0.435	0.518	0.054	0.387	0.539	0.055	0.381	0.541
	2	**6**b	0.704	0.137	0.068	0.482	0.239	0.192	0.638	0.158	0.075

[a] Spin densities determined by Mulliken population analysis. [b] Geometries were optimized at the B3LYP/TZVP level of theory.

The spin distribution can be substantially influenced by the amount of the Hartree−Fock (HF) exchange interaction in the hybrid functional.[37] We have chosen the B3LYP functional because we have previously found a good correlation between the experimental infrared spectra of various copper(II)/phenoxy ions and the B3LYP calculated spectra.[23,24,38] Here, we have investigated the effect of the variation of the HF exchange by single-point calculations at the B38P86/TZVP[37a] (38% of the HF exchange) and BHandHLYP/TZVP (50% of the HF exchange) levels, respectively, for the B3LYP/TZVP optimized structures (Table 5). The increasing amount of the HF exchange leads to a more localized spin population. Thus, the spin is more localized either at the phenoxy ligand or at the copper. We have further reoptimized the geometries of all complexes at the B38P86 level, which for complexes containing copper(II) (**3**b_2 and **6**b) led to even larger localization of the spin at the copper ion. Thus, the calculations show analogous results, only the transition between copper(I) and copper(II) complexes is more sharp.

Summary and Conclusions

In a previous work we have shown that the complex $[Cu(PhO)(PhOH)]^+$ is composed of Cu(I), a phenoxy radical ligand, and neutral phenol, which preferentially coordinates copper via its aromatic π system.[23] As an extension of this work we have here investigated the effects of additional ligand coordination to the $[Cu(PhO)(PhOH)]^+$ core. In a combined quantum chemical and mass-spectrometric study of $[Cu(PhO)L]^+$ complexes with various donor ligands L we found an increase of binding energies in the order H_2O < CH_3OH < THF < NH_3 < pyridine < imidazole. We have shown that the nature of the ligands introduced primarily influences the charge distribution in the complex, and we have observed a linear dependence of the binding energies of monodentate ligands L and the charge localization at the PhO ligand. The same trend is also observed for the $[Cu(PhO)(PhOH)L_n]^+$ complexes (L = H_2O, NH_3, and 4-methylimidazole; n = 1, 2). With an increasing binding energy in the order H_2O < NH_3 < Imi_{Me}, ligand addition has an increasing effect on the molecular and electronic structures of the resulting complexes.

The σ-coordination mode of phenol in $[Cu(PhO)(PhOH)L_n]^+$ is continuously stabilized with respect to the π-coordination mode along the series of ligands H_2O − NH_3 − 4-methylimidazole, but only in the $[Cu(PhO)(PhOH)(Imi_{Me})_2]^+$ complex is the σ-coordination clearly preferred. The change in the preferred coordination mode is associated with the shift between oxidation states I and II, which can be straightforwardly probed by the C═O stretching frequency of the PhO ligand, which changes from 1500 cm^{-1} in free phenoxy to around 1300 cm^{-1} for the Cu(II)/phenolate complexes.

Our investigations on this simple model indicate that the immediate ligand environment of the metal intrinsically determines coordination modes and electronic characteristics of copper radical oxidases binding sites. While the coordination geometry of the $[Cu(PhO)(PhOH)]^+$ core are flexible and easily modified by inclusion of any additional donor ligand in the Cu coordination shell, addition of two imidazole ligands strictly determines the coordination geometry. Thus, in agreement with known structures of active sites containing copper coordinated by tyrosine and histidine groups, we have shown that coordination of 4-methylimidazole ligands to the $[Cu(PhO)(PhOH)]^+$ core leads to complexes, in which all ligands are coordinated via heteroatoms.

Here, we have shown that the interaction between copper(II) and phenol/phenolate ligands, which are found often in active centers of biomolecules, crucially depends on the number and nature of additional ligands coordinated to copper. Our findings demonstrate that for the design of small models of metal-containing active centers of biomolecules or processes in the condensed phase, it is essential to correctly mimic the coordination environment of the metal. Small changes in the coordination geometry of model complexes can in fact lead to dramatic changes of the metal ion properties as well as of the properties of coordinated ligands. Thus, while the number of ligands influences the spin distribution in the complexes, the nature of the ligands influences the charge distribution and binding energies between metal and ligands.

Acknowledgment. The authors thank Prof. Peter Chen for providing the L-CID program. This work was

(37) For examination of the HF exchange correlation on the spin distribution in copper complexes see: (a) Szilagyi, R. K.; Metz, M.; Solomon, E. I. *J. Phys. Chem. A* **2002**, *106*, 2994. (b) Atanasov, M.; Comba, P.; Martin, B.; Müller, V.; Rajaraman, G.; Rohwer, H.; Wunderlich, S. *J. Comput. Chem.* **2006**, *27*, 1263. (c) Saito, T.; Kataoka, Y.; Nakanishi, Y.; Matsui, T.; Kitagawa, Y.; Kawakami, T.; Okumura, M.; Yamaguchi, K. *Chem. Phys.* **2010**, *368*, 1.

(38) Roithova, J.; Milko, P. *J. Am. Chem. Soc.* **2010**, *132*, 281.

supported by the Grant Agency of the Academy of Sciences of the Czech Republic (KJB400550704), Grant agency of the Czech Republic (203/08/1487), the Ministry of Education of the Czech Republic (MSM0021620857), and the Deutsche Forschungsgemeinschaft (TR-SFB 49, project B5). We gratefully acknowledge support by the Frankfurt Center for Scientific Computing and HHLR Darmstadt.

Supporting Information Available: Further details are given in Table S1 and Figures S1−S14. This material is available free of charge via the Internet at http://pubs.acs.org.